Metaheuristic Quantum Glowworm Swarm Optimization based Clustering With Secure Routing Protocol for Mobile Adhoc Networks

Srinivas Maganti (srinivas.maganti@vrsiddhartha.ac.in)
VR Siddhartha Engineering College: Velagapudi Ramakrishna Siddhartha Engineering College
M.Ramesh Patnaik
Andhra University

Research Article

Keywords: Wireless Sensor Networks, Clustering, Routing, Gravitational Search Algorithm, Glowworm Swarm Optimization, Metaheuristics

Posted Date: March 26th, 2021

DOI: https://doi.org/10.21203/rs.3.rs-266082/v1

Metaheuristic Quantum Glowworm Swarm Optimization based Clustering with Secure Routing Protocol for Mobile Adhoc Networks

Maganti Srinivas[1,*] Dr.M.Ramesh Patnaik[2]

[1]Research Scholar/Instrument technology, A.U.College of Engineering, Andhra University, Visakhapatnam, Andhra Pradesh 530003, India

[1]Assistant Professor/EIE, V.R.Siddhartha Engineering College, Vijayawada, Andhra Pradesh 520007 India

[2]Associate Professor/Instrument technology, A.U.College of Engineering, Andhra University, Visakhapatnam, Andhra Pradesh 530003, India

[1,*]srinivas.maganti@vrsiddhartha.ac.in [2]ramesh_patnaik@yahoo.com

Abstract

Mobile adhoc network (MANETs) comprises a collection of independent, compact sized, and inexpensive sensor nodes, which are commonly used to sense the physical parameters in the geographical location and transmit it to the base station (BS). Since clustering and routing are considered as the commonly used energy efficient techniques, several metaheuristic algorithms have been employed to determine optimal cluster heads (CHs) and routes to destination. But most of the metaheuristic techniques have failed to achieve effective clustering and routing solutions in large search space and the chance of generating optimal solutions is also considerably reduced. To resolve these issues, this paper presents a new Metaheuristic Quantum Glowworm Swarm Optimization based Clustering with Secure Routing Protocol for MANET, named QGSOC-SRP. The presented QGSOC-SRP technique follows two stage processes, namely optimal CH selection and route selection. Firstly, the QGSO algorithm derives a fitness function using four variables such as energy, distance, node degree, and trust factor for optimal election of secure CHs. Secondly, the SRP using oppositional gravitational search algorithm (OGSA) is applied for the optimal selection of routes to BS. The traditional GSA is inspired by the law of gravity and interaction among masses. To improve the effectiveness of the GSA, OGSA is derived based on the oppositional based learning concept for population initialization and generation jumping. For validating the effective results of the presented OGSOC-SRP technique, a set of experiments were performed and the results are determined interms of distinct measures.

Keywords: Wireless Sensor Networks, Clustering, Routing, Gravitational Search Algorithm, Glowworm Swarm Optimization, Metaheuristics

1. Introduction

In general, Mobile Ad Hoc Network (MANET) is a multi-hop transitory as well as self-sufficient system configured by mobile nodes and wireless connections [1]. In MANET, a node is capable to join and relieve from a system dynamically [2]. Due to the scalable and infrastructure less behavior of MANET, it is employed in military services and alternate civilian applications. The key objective of MANET is to exchange information among rescuers, searching teams, and clinical professionals, especially in emergency sites in case of complete network failure [3]. Also, various other habitats in routine life such as weather forecasting, ocean tracking, traveler location, destination monitoring, and social network [4]. Using the closer range space and rapid deployment of airliner like drones, MANETs are composed of high diversity. But, MANETs are limited with insufficient speed limit of battery, and energy which is still a complicated problem for various applications [5]. For inadequate power of MANET, developing a routing protocol is to ensure the extensive convergence, and improve the efficiency of novel routes. Additionally, it is significant to enhance the power utilization and make sure an effective data transmission, and which modifies the aggressive changes processed by network topology.

Numerous traditional models have been employed on energy equalizing protocols. Usage of effective energy mechanism intends to mitigate the power application and improvise the system duration. Typically, the protocols are divided into 2 categories: low energy and maximum network lifetime routing protocols. First, routing protocols with low power identifies a power effective routing path from source to target [6] while improvised network lifetime manages to balance the node power and explore energy-saving router [7]. Additionally, ant colony mechanism performs well by means of power management and is extensively used in multiple domains. Next, a bionic concept mimics the character of living organisms on Earth. The major objective of this method is to achieve optimal results with minimum power resources. Mostly, it is employed to enclose simple heuristic approaches within dispersed tasks [8]. The Ant Colony Optimization (ACO) method contains massive benefits and features. Actually, ACO is a new heuristic approach used for resolving integrated optimizing problems. Few characteristics of ACO are positive feedback, distributed processing, and dynamic changes [9].

Baras and Mehta [10] deployed Probabilistic Emergent Routing Algorithm (PERA). The extended version of ACO for MANET is referred as PACONET as defined in [11] applies

forward and backward ants to increase the pheromone level that is different from AntNet concept. Initially, forward ant enhances pheromone to maximize the convergence of a system and results in trapping within local optimum issues. It is composed of maximum broadcast as each ant needs time for discovering path and ID of previous nodes. In order to overcome these problems, a basic ACO gets easily trapped within the local optimum, and Bullnheimer et al. [12] presented a Rank-Based Version of Ant System (ASrank). It is projected by developing a mechanism of sorting in Genetic Algorithm (GA).

Woungang et al. [13] established ant-swarm based energy-effective ad hoc on-demand routing protocol (ACO-EEAODR) by means of RE and router length of a node. Here, weighting factors of 2 characteristics in a protocol gain various metrics according to different cases, whereas pheromones of each node are expanded over residual energy (RE). In de Figueiredo Marques et al. [14], ACO is utilized in mesh routing system to identify best routes while managing shared coordination among nodes with Low-Power and Lossy network (LNNs) with minimum energy application. Now, ACO is named LNNACO which enhances the transmission rate by considering the power utilization in Max-Min-Path(MMP) ACO method. Since the LNNACO method is unable to identify the effect of maximum mobility and it is unfit for high speed networks.

In Zhou et al. [15], AC based Energy Control Routing Protocol (ACECR) has been presented. It considers maximum and minimum RE for each path. For route discovery, backward ant upgrading is enabled and pheromone table is based on minimum power and hop count. However, ACECR is unable to make sure the complete transmission energy can be limited with defined router. Mohsen[16] utilized Simulated Annealing (SA) concept for identifying global optimal path, by the combination of SA and ACO. Some of the existing models are time consuming by means of computing the routing path and distance of a router is maximum when compared with ACO approach.

This paper introduces a novel Metaheuristic Quantum Glowworm Swarm Optimization based Clustering with Secure Routing Protocol for MANET, named QGSOC-SRP. The presented QGSOC-SRP technique involves OGSO based optimal CH selection and SRP based route selection. The SRP using oppositional gravitational search algorithm (OGSA) is applied for the optimal selection of routes to BS. To improve the effectiveness of the GSA, OGSA is derived based on the oppositional based learning concept for population initialization and

generation jumping. The experimental validation of the presented model takes place in different aspects.

2. The Proposed QGSOC-SRP technique

The workflow involved in the presented QGSOC-SRP method is depicted in Fig. 1. Consider a MANET with ‘n’ mobile sensor placed randomly wherever required. A sensor node is deployed and begins to collect information reading the surrounding environment. Then, the QGSOC algorithm gets executed by the Base station (BS) to elect the cluster heads (CHs) by the use of a fitness function (FF) involving four variables such as energy, distance, node degree (ND), and trust factor for optimal election of secure CHs. Followed by, OGSA based routing technique is applied to pick up an optimal path to BS. Finally, the data will be transmitted from cluster members (CMs) to CHs and thereby to BS.

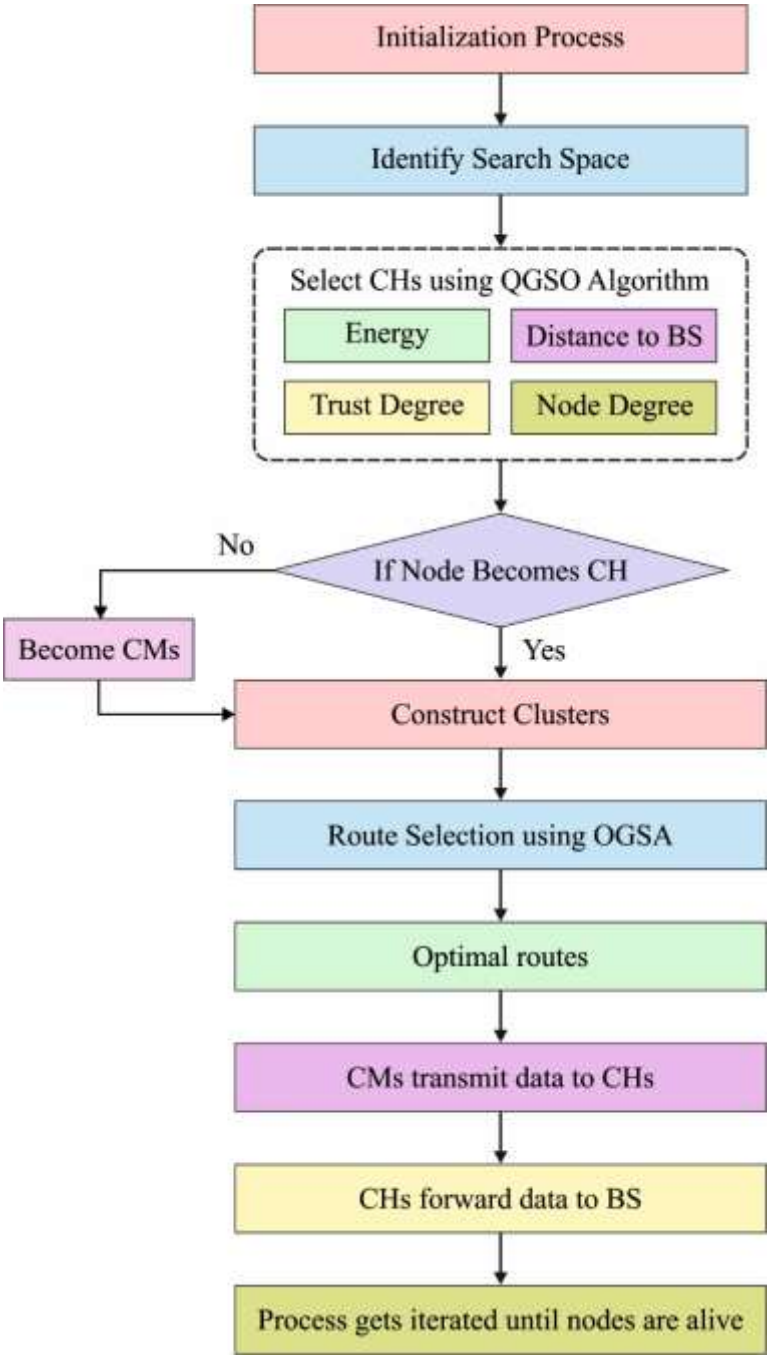

Fig. 1. Work flow of QGSOC-SRP model

2.1. QGSOC Technique

Here, the detailed performance of QGSO algorithm based clustering process and the optimal election of CHs are provided clearly.

2.1.1. Glowworm swarm optimization (GSO)

Usually, GSO is considered as modern swarm optimization method evolved from the luminescent feature of fireflies. Here, the glowworm swarms are distributed in a solution space as well as fluorescence intensities are relevant to the FF of glowworm's location. The position of a glowworm depends upon the intensity of brightness which means the FF values are maximum. Also, glowworms have a dynamic line of vision, which is referred as decision domain, where the range is relevant to density of adjacent nodes. Once the maximum number of iterations is reached, the glowworms are placed in best locations [17]. Typically, this method is composed of 5 phases namely, upgrading the fluorescein concentration, increment in neighbor set, enhance the decision domain radius, update moving probability, and upgrade glowworm position. Hence, fluorescein concentration increment mechanism is classified by Eq. (1).

$$l_{\mathrm{i}}(\mathrm{t}) = (1-\alpha) l_i(t-1) + \beta f\big(x_{\mathrm{i}}(\mathrm{t})\big), \tag{1}$$

where $l_i(\mathrm{t})$ implies fluorescein concentration of ith glowworm at time f, α means the fluorescein volatilization coefficient, β denotes the fluorescein enhancing factor, $f(x)$ refers the FF value and $x_i(\mathrm{t})$ defines the location of glowworm i at t time. Therefore, increment in neighbor set is defined by

$$N_i(\mathrm{t}) = \big\{j: \big\|\chi_j(\mathrm{t}) - x_i(\mathrm{t})\big\| < r_d^{\mathrm{i}}; l_{\mathrm{i}}(\mathrm{f}) < l_j(\mathrm{t})\big\}, \tag{2}$$

where $N_i(\mathrm{t})$ refers the neighbor set of ith glowworm at time t as well as $r_{\mathrm{d}}^i(t)$ mimics the radius of decision domain of ith glowworm at moment t. Thus, enhancing decision domain radius mechanism is illustrated in Eq. (3).

$$r_d^{\mathrm{i}}(\mathrm{t}+1) = \min\Big\{r_s, \quad \max\big\{r_d^i(\mathrm{t}) + \gamma(n_{\mathrm{i}} - |N_i(\mathrm{r})|)\big\}\Big\}, \tag{3}$$

Where r_s denotes the perceived radius of glowworm, γ implies the rate of change of decision domain, and n_i signifies the adjacent threshold. As a result, update moving probability of a framework is demonstrated in Eq. (4).

$$Pij(\mathrm{t}) = \frac{l_j(t) - l_{\mathrm{i}}(\mathrm{t})}{\sum_{\mathrm{k}\in N_t} l_k\,(\mathrm{t}) - 1_i(t)}, \tag{4}$$

Where $p_{ij}(\mathrm{t})$ implies the probability with glowworm i moves to glowworm j at time t. The upgrade glowworm position mechanism is depicted in Eq. (5).

$$x_i(\mathrm{t}+1) = x_i(\mathrm{t}) + s\left(\frac{x_j(\mathrm{t}) - x_i(t)}{\|x_j(\mathrm{t}) - x_i(t)\|}\right), \tag{5}$$

For enhancing the working function of GSO method, quantum computing is incorporated. Fig. 2 illustrates the flowchart of GSO model.

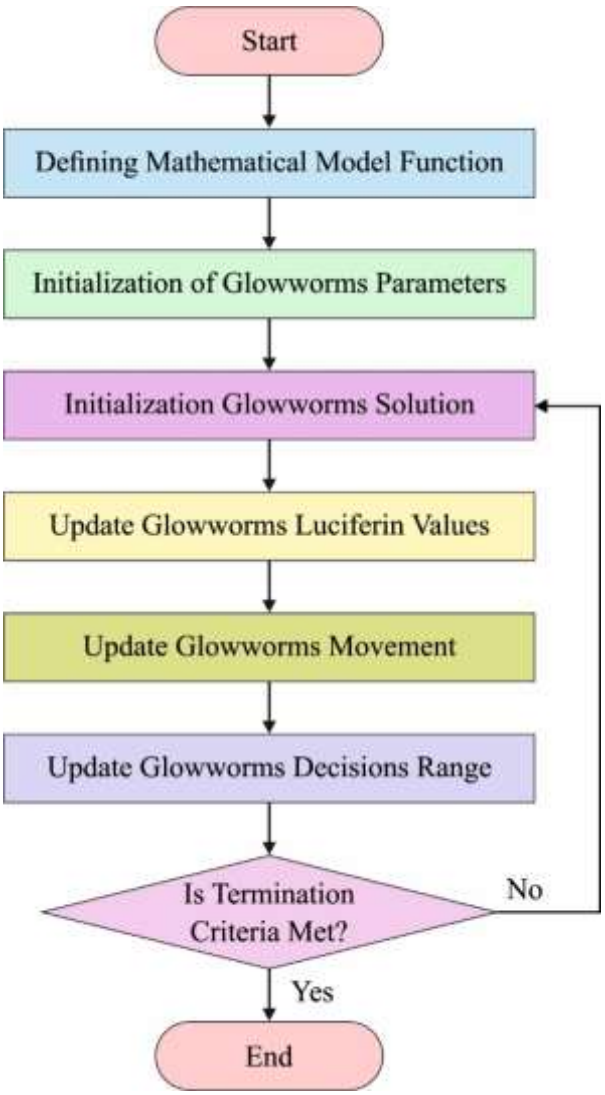

Fig. 2. Flowchart of GSO algorithm

2.1.2. Quantum GSO Algorithm

Quantum computing is considered as a computation model which employs the relevant mechanism to quantum theory like quantum estimation, state superposition, as well as quantum entanglement. The basic unit of quantum processing is qubit. The basic states $|0>$ and $|1>$develops a qubit which is illustrated as linear combination of 2 fundamental states as shown in the following,

$$|Q>=\alpha|0>+\beta|1>. \quad (6)$$

$|\alpha|^2$ defines the possibility of observing state $|0>$, $|\beta|^2$ implies the possibility of observing state $|1>$, in which $|\alpha|^2+|\beta|^2=1$. A quantum is deployed with the help of n qubits. Due to the quantum superposition, a quantum is comprised of 2^n possible metrics. Finally, n-qubits quantum is demonstrated as provided in the following.

$$\Psi=\sum_{x=0}^{2^n-1} C_x|x>, \sum_{x=0}^{2^n-1}|C_x|^2=1. \quad (7)$$

The condition of qubits like rotation gate, NOT gate, Hadamard gate,are modified using quantum gtaes. Initially, rotation gate [18] is defined as a mutation operator used for developing quanta mechanism and best solutions to identify an global optimal solution.

The rotation gate is illustrated as follows:

$$\begin{bmatrix}\alpha^d(t+1)\\ \beta^d(t+1)\end{bmatrix}=\begin{bmatrix}\cos(\triangle\theta^d) & -sin(\triangle\theta^d)\\ sin(\triangle\theta^d) & cos(\triangle\theta^d)\end{bmatrix}\begin{bmatrix}\alpha^d(t)\\ \beta^d(t)\end{bmatrix} for\ d=1,2,\dots,n. \quad (8)$$

$\triangle\theta^d=\triangle\times S(\alpha^d,\beta^d)$, $\triangle\theta^d$ signifies the rotation angle of qubit, where $\triangle$ and $S(\alpha^d,\beta^d)$ refers the size and dimension of rotation respectively.

2.1.3. QGSO based CH Selection Process

The FF of QGSO is applicable in resolving the optimal clustering issues. Due to the complicated nature, maximum control data has to be replaced between the nodes in CH election, which results in system overhead. In order to overcome this issue, QGSO FF has been applied. Also, the local density of CH and average distance inside a cluster, power utilization of nodes, and dispensability of CH are some of the parameters used in controlling the generation of unequal network clustering.

In CH election phase, distribute CH, eliminate missing data, develop adjacent node to join CH and power utilization is higher than CM nodes. With no balancing metrics, the premature death of CH occurs and power drain rapidly. The major node in a system is assumed to be CH. Thus, the position of CH has to be determined and to reduce the size of CH nearby sink or BS nodes, where multiple CH accounts for data forwarding process and increase the real-time process and power utilization of CH.

Consider N nodes for developing K clusters with M(K $<<$ M) candidate CH. Followed by, a network is composed of C_n^k clustering models and select best clustering mechanism are referred as optimization issues. Under the application of GSO FF, the optimal clustering issues can be resolved and FF assumes local density of CH, average distance inside a cluster, and energy dispersion of nodes.

Assume a WSN with N sensor nodes and develop K clusters [19]. The CH election is performed by using QGSO FF to resolve the clustering issues. Hence, FF is obtained using 5 input attributes like RE, communication expense, trust degree, ND as well as node marginality.

$$f(x) = \varepsilon 1\, f1(pj) + \varepsilon 2\, f2(pj) + \varepsilon 3\, f3(pj) + \varepsilon 4\, f4(pj) + \varepsilon 4\, f5(pj) \quad (9)$$

Where f1-f5 implies the 5 attributes defined above.

2.1.3.1. Residual energy

It is a significant parameter applied in WSN. Here, CHs need high power than CMS because of processing aggregation, computation, and data routing. Therefore, RE is evaluated by using applied expression:

$$E_r = E_0 - E_c \quad (10)$$

where E_0 and E_c denotes the basic energy and power used by nodes, respectively; and E_r indicates the RE of regular node.

2.1.3.2. Communication cost

The forwarding data has observed energy which is directly proportional to square of distance among 2 nodes. The count of processing cost is demonstrated as given below:

$$C = \frac{d_{avg}^2}{d_0^2}, \quad (11)$$

Where d_{avg} signifies the high distance between a node and neighbors; d_0 refers the broadcasting radius of a node.

2.1.3.3. Trust degree

Basically, a node is assigned to triangle function (TF) value 1. Next, value of TF is restricted by independent prediction concept whereas a node process anomalous operation and node is decided as anxious node and TF nodes are demonstrated in Eq. (12):

$$\mathrm{TF}_x = \begin{cases} Normal, & 0.8 \le T_i < 1 \\ Suspected, & 0.3 \le T_i < 0.8 \\ Malicious, & 1 \le T_i < 0.3 \end{cases} \tag{12}$$

Here, nodes with TF_x modifies the opportunity of becoming CHs. When the node falls under TF_x of malicious node, it is removed from cluster and suspicious nodes are considered as CM and not as CH.

2.1.3.4. Node degree

The rule applied in ND is that nearby neighbors model has optimal measure; a node with maximum probability is declared as CH. Hence, ND is computed as given below:

$$D = \frac{|D_i - D_0|}{D_0}. \tag{13}$$

Where, D_j defines the measure of neighboring nodes and D_0 implies the optimal number of neighbors.

2.2. OGSA based SRP

Once the CHs are chosen, the subsequent process is to elect an optimal set of CHs. It is performed by the use of OGSA. The detailed working of the OGSA based route selection process is defined here.

2.2.1. Overview of GSA

Generally, GSA [20] is composed of agents which are assumed as objects and performances validation is carried out by using the masses. The objects are attractedto one another by gravitational force where the global objects move around the global movement of objects with heavyweights. Therefore, masses cooperate with the help of various communication by gravitational force. The weighted masses move slowly when compared with light-weighted objects. As a result, it makes sure the exploitation of a model.

In GSA is mass or agent is composed of 4 specifications namely, position, inertial mass, active and passive gravitational mass. Initially, position of a mass refers a solution to the

problem, and gravitational as well as inertial masses can be estimated under the application of FF value. Besides, a mass is considered to be a solution. Also, it is directed by an appropriate modification of gravitational, and inertial masses. As a result, optimal solution might be gained in a search space. Mostly, the given rules are followed by the masses.

i. Law of gravity: A particle attracts the adjacent particles by the existence of gravitational force among 2 particles are directly proportional to product of masses and inversely proportional to square of distance (R). R is employed as an alternative toR^2 since R has provided considerable outcome when compared with R^2 with standard test functions.
ii. Law of motion: The recent velocity of a mass is similar to summation of fractions from existing velocities and differences in the velocity.

Then, assume a model with n agents. Also, location of ith agent is depicted by:

$$X_i = \left(x_i^1, \ldots, x_i^d, \ldots, x_i^n\right) for\ i = 1,2, \ldots, n \tag{14}$$

Where x_i^d denotes the location of ith agent in dth dimension. At time t, force employed on ith mass from jth mass is described as shown the following expression,

$$F_{ij}^d(t) = G(t) \times \frac{M_{pasi}(t) \times M_{actj}(t)}{R_{ij}(t) + \varepsilon} \times \left(x_j^d(t) - x_i^d(t)\right) \tag{15}$$

where $M_{actj}(t)$ and $M_{pasi}(t)$ depicts the active as well as passive gravitational mass relevant to jth and ith agent at time $t, G(t)$ shows a gravitational constant at time t, ε refers a minimum constant, and $R_{ij}(t)$ signifies the Euclidian distance among 2 agents i and j as expressed in the following,

$$R_{ij}(t) = \left\|X_i(t), X_j(t)\right\|_2 \tag{16}$$

In order to provide a stochastic feature, it is desired that the overall force applied on ith agent in dth dimension is randomly weighted sum of dth elements of forces released from alternate agents represented by given function:

$$F_i^d(t) = \sum_{j=1, j \neq i}^{N} rand_j \times F_{ij}^d(t) \tag{17}$$

where $rand_j$ denotes a random value from [0,1]. Therefore, using law of motion, the simulation of ith agent at time t in dth dimension is illustrated by the given expression:

$$acc_i^d(t) = \frac{F_i^d(t)}{M_{inti}(t)} \tag{18}$$

where $M_{\text{int}i}(t)$ depicts the inertial mass of ith agent. The position and velocity of an agent could be measured by using given expression.

$$v_i^d(t+1) = rand_i \times v_i^d(t+1) + acc_i^d(t) \tag{19}$$

$$x_i^d(t+1) = x_i^d(t) + v_i^d(t+1) \tag{20}$$

In (19), $rand_i$ implies an equal random variable from [0, 1]. The random value is employed for generating randomized features. The gravitational constant (G) is accelerated and limited with time for controlling the exploring accuracy. On the other hand, Gsignifies a function of basic value (G_0) and time (t) is demonstrated as shown below:

$$G(t) = G\left(G_{0,t}\right) = G(t_0) \times \left(\frac{t_0}{t}\right)^A A < 1 \tag{21}$$

In (21), $G(t)$ refers the score of gravitational constant at time $t, G(t_0)$ defines the measure of gravitational constant at cosmic quantum interval of time t_0. Then, $G(t)$ is fixed using the given expression:

$$G(t) = G_0 \times e^{-\tau\left(\frac{iter}{iter_{max}}\right)} \tag{22}$$

where G_0 is allocated to 100, s is declared to 20, $iter$ and $iter_{\max}$ demonstrates the recent and overall count of iterations correspondingly. Gravitational and inertia masses are determined using the fitness estimation. By considering the uniformity of gravitational mass and inertia mass, the scores of masses are determined with the help of fitness mapping and it is upgraded by given expressions:

$$M_{acti} = M_{pasi} = M_{\text{int}i}\ for\ 1,2,\dots,n \tag{23}$$

$$m_i(t) = \frac{fit_i(t) - worst(t)}{best(t) - worst(t)} \tag{24}$$

$$M_i(t) = \frac{m_i(t)}{\sum_1^N m_i(t)} \tag{25}$$

Where $fit_i(t)$ demonstrates the fitness measure of ith agent at time t, and $worst(t)$ as well as $best(t)$ are illustrated in (26) and (27), correspondingly, for minimization issues.

$$best(t) = \min_{j\in\{1,\ldots,n\}} fit_j(t) \tag{26}$$

$$worst(t) = \max_{j\in\{1,\ldots,n\}} fit_j(t) \tag{27}$$

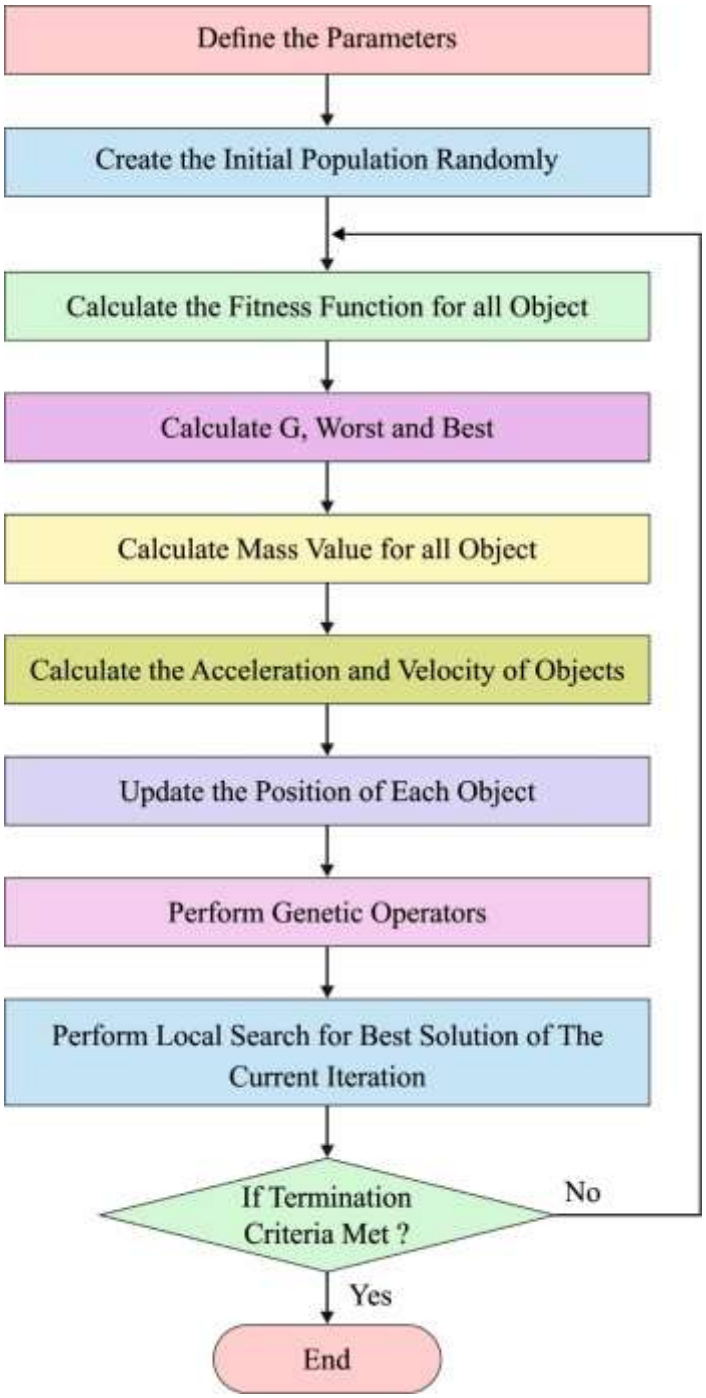

Fig. 3. Flowchart of GSA algorithm

This rule is applied significantly as it is capable of reducing the exploration ability and enhance the exploitation quality. Fig. 3 demonstrates the flowchart of GSA method. To eliminate the trapping within local optimum, the method has to apply exploration initially. In most of the iterations, exploration should fade out and exploitation should fade in. In order to enhance the working function of GSA, managing exploration and exploitation by $Kbest$ agents attract the adjacent masses. $Kbest$ is defined as a function of time with fundamental measures K_0 and it reduces with time. Followed by, every agent employs the forces initially, and, $Kbest$ is reduced in linear fashion. Hence, Eq. (22) can be extended as,

$$F_i^d(t) = \sum_{j \in Kbest, j \neq i} rand_j \times F_{ij}^d(t) \tag{28}$$

In (28), $Kbest$ refers the group of K agents with optimal fitness measures and heavier masses.

2.2.2. Opposition-based learning

Evolutionary optimization models initiates few solutions and attempts to maximize the supremacy of optimal solution(s). The process of exploration is terminated if predefined condition is fulfilled. Under the inexistence of *apriori* data, it is often initialized with random guesses. Hence, processing time is related to distance of initial guesses from optimal solution. The chance of simulating fitter solution is improved by validating the opposite solution [21]. Followed by, the closer object is considered to be a primary solution. Similarly, the method is employed to initial and current solution in a search space.

Consider $x \in [a, b]$ as a real value. The opposite value is illustrated by

$$\breve{x} = a + b - x \tag{29}$$

Assume $P = (x_1, x_2, \ldots, x_d)$ as a point in d-dimensional space, in which $x_1, x_2, \ldots, x_\mathrm{d} \in R$ and $x_i \in [a_\mathrm{i}, b_i] \forall_i \in \{1, 2, \ldots, d\}$. The opposite point $\breve{P} = (\breve{x}_1, \breve{x}_2, \ldots, \breve{x}_d)$ is described by the elements as shown below,

$$\breve{x}_i = a_i + b_i - x_i \tag{30}$$

Then, using the opposite point statement, opposition-based optimization is illustrated as follows.

Suppose $P = (x_1, x_2, \ldots, x_d)$ is a point in d-dimensional space, then consider $f = (\cdot)$ is a FF applied for measuring the candidate's fitness value. Based on the description of opposite point, $\breve{P} = (\breve{x}_1, \breve{x}_2, \ldots, \breve{x}_d)$ is referred as opposite value of $P = (x_1, x_2, \ldots, x_d)$. Next, when $f(\breve{P}) \geq f(P)$, then point P is interchanged with $\breve{P}$; else, it is repeated.

2.2.3. Opposition-based gravitational search algorithm

Alike the population-based optimization approaches, 2 major steps are differentiable for GSA, like population initialization and make new generations using GSA. Recently, the principle of OBL is embedded in 2 phases [22]. The actual GSA is selected as parent model and opposition-based procedures are incorporated with the aid of implementing simulated convergence profile.

2.2.4. QGSA based Route Selection Process

Here, the newly developed OGSA based routing method has been defined for computing efficient routing process applies a heuristic mechanism. When compared with other heuristic models, this approach provides optimal solution for identifying optimal route for reducing power consumption.

In this framework, system with 'N' count of CHs are assumed and ith CH place is depicted by Eq. (31).

$$\mathrm{y}_i = \left(y_i^1, \ldots, y_i^d, \ldots, y_i^n\right) for\ i = \ 1, 2, 3, \cdots N \tag{31}$$

At time t, force applied on ith CH from jth CH along with static mass is demonstrated in Eq. (32).

$$F_{ij}^{(t)} = \frac{g(t)}{D_{ij}(t) + \mu}\left[y_j^d(t) - y_i^d(t)\right] \tag{32}$$

where μ denotes the simple constant, g(t) indicates the gravitational force at time 't', and $D_{ij}(t)$ refers Euclidean distance from node 'i' and node 'j'.

$$D_{ij}(t) = \|y_i(t), y_j(t)\|_2 \tag{33}$$

The overall force employed on ith CH exerted from alternate CH with d dimension is assumed to be weighted sum of force acting from adjacent CH is depicted in Eq. (34).

$$F_i^d(t) = \sum_{j=1 j \neq i}^{N} F_{ij}^d(t) \quad (34)$$

Based on the law of motion, acceleration is triggered by force. If mass is constant, then the acceleration is presented for overall force applied on ith CH to 'jth' CH. In this model, acceleration of CH 'i' at 't' time is presented in Eq. (35).

$$a_i^d(t) = \frac{F_i^d(t)}{m(t)}, where\ m(t) = 1 \quad (35)$$

The CH election is carried out randomly. Hence, velocity and position of CH should be determined [23]. Also, velocity of CH at time $t + 1$ is processed by the recent velocity along with the acceleration. Therefore, upcoming position of 'ith' CH and corresponding velocity is evaluated by Eqs. (36) and (37).

$$V_i^d(t+1) = V_i^d(t) + a_i^d(t) \quad (36)$$

$$Y_i^d(t+1) = y_i^d(t) + V_i^d(t+1) \quad (37)$$

It is used in finding the optimal route between alternate routes. When best route is not found then follow the same process until reaching the termination criteria.

3. Performance Validation

Table 1 shows the analysis of the results attained by the QGSOC-SRP method under different speed of mobile nodes. Fig. 4 illustrates the count of CH changes under varying mobile node speed by the QGSOC-SRP and previous methods. From the figure, it is clear that the QGSOC-SRP approach has resulted in optimal performance when compared with alternate approaches by gaining least number of CH changes irrespective of the mobile node speed. For sample, under the application of a mobile node speed of 2m/s, the QGSOC-SRP framework has demonstrated 6 CH changes while the FUCHAR, COMBA, and EMPSO have generated maximum CH changes of 9, 10, and 12 correspondingly. Simultaneously, under the existence of a mobile node speed of 6m/s, the QGSOC-SRP framework has illustrated only 8 CH changes whereas the FUCHAR, COMBA, and EMPSO have offered high CH changes of 12, 15, and 20 respectively. Meantime, under the existence of a mobile node speed of 10m/s, the QGSOC-SRP approach has depicted only 8 CH changes while the FUCHAR, COMBA, and EMPSO have obtained supreme CH changes of 10, 14, and 17 respectively.

Table 1 Results analysis of QGSOC-SRP Technique under varying speed of mobile nodes

Number of Cluster Head Changes				
Mobile Node Speed (m/s)	QGSOC-SRP	FUCHAR	COBMA	EMPSO
2	06.00	09.00	10.00	12.00
4	05.00	07.00	09.00	14.00
6	08.00	12.00	15.00	20.00
8	13.00	22.00	24.00	26.00
10	08.00	10.00	14.00	17.00
Number of Cluster Member Changes				
Mobile Node Speed (m/s)	QGSOC-SRP	FUCHAR	COBMA	EMPSO
2	31.00	45.00	47.00	49.00
4	26.00	42.00	45.00	48.00
6	24.00	47.00	49.00	52.00
8	25.00	51.00	54.00	56.00
10	20.00	50.00	52.00	53.00

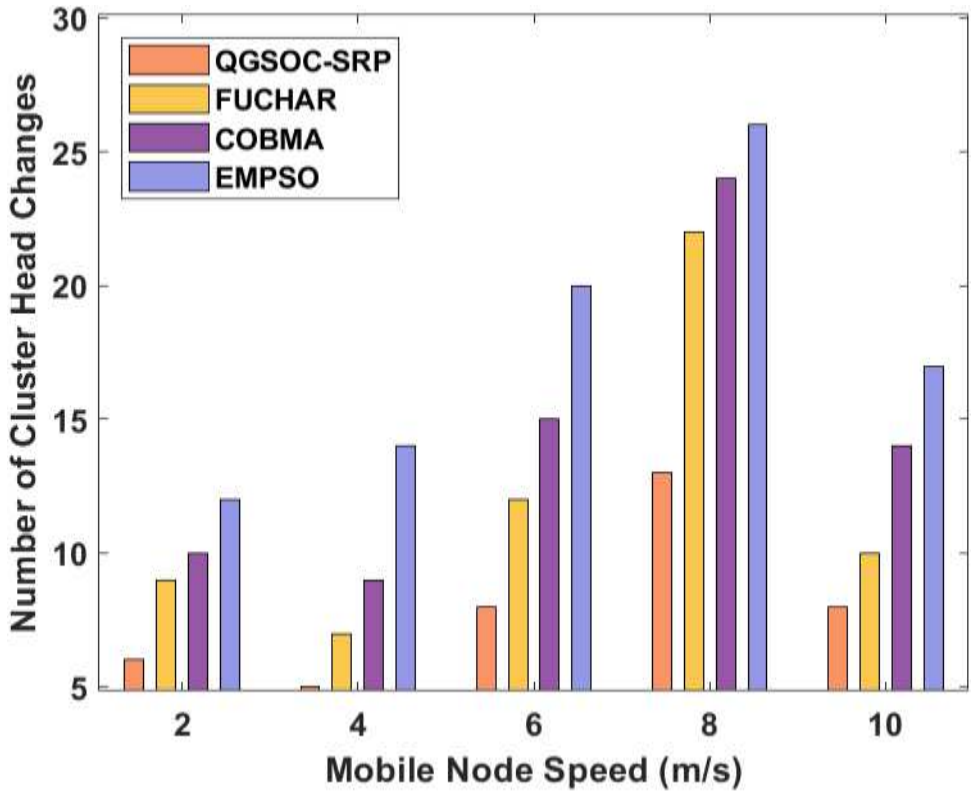

Fig. 4. Results analysis of QGSOC-SRP model in number of cluster head

Fig. 5 demonstrates the number of CM changes under different mobile node speeds by the QGSOC-SRP and classical models. From the figure, it is illustrated that the QGSOC-SRP scheme has provided optimal function over the alternate models by accomplishing limited number of CM changes irrespective of mobile node speed. For example, under the application of a mobile node speed of 2m/s, the QGSOC-SRP scheme has showcased only 31 CM changes while the FUCHAR, COMBA, and EMPSO have concluded in a maximum CM changes to 45, 47, and 49 respectively. Concurrently, under the existence of a mobile node speed of 6m/s, the QGSOC-SRP framework has displayed 24 CM changes and the FUCHAR, COMBA, and EMPSO have projected high CM changes of 47, 49, and 52 correspondingly. At the same time, using a mobile node speed of 10m/s, the QGSOC-SRP model has illustrated 20 CM changes and FUCHAR, COMBA, and EMPSO have implied maximum CM changes of 50, 52, and 53 respectively.

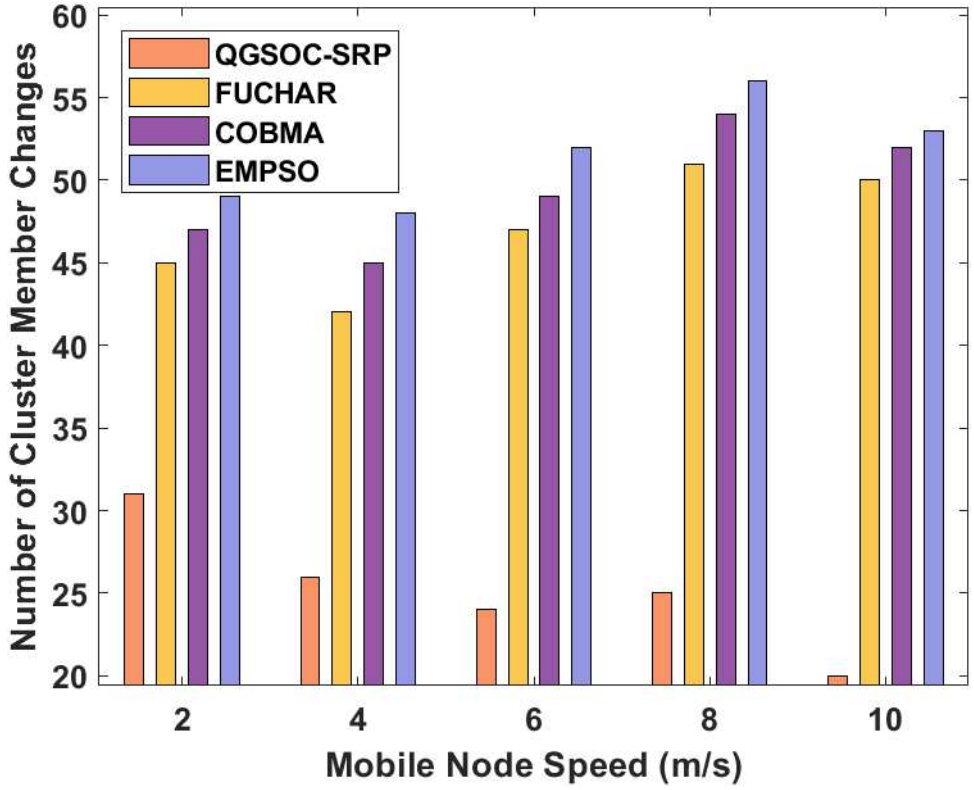

Fig. 5. Results analysis of QGSOC-SRP model in number of cluster member

Table 2 offers an extensive results analysis of the QGSOC-SRP model under varying number of mobile nodes. Fig. 6 investigates the EC analysis of the QGSOC-SRP model under diverse mobile nodes. The figure reported that the EMPSO algorithm has shown inferior outcomes by exhibited maximum EC. In line with, the FUCHAR and COMBA models have demonstrated somewhat reasonable outcome by offering slightly lower EC over the EMPSO algorithm.

Table 2 Result Analysis of Existing with Proposed QGSOC-SRP Method in terms of Various Parameters

No. of Mobile Nodes	**Energy Consumption (EC) (mJ)**			
	QGSOC-SRP	FUCHAR	COBMA	EMPSO
100	31	45	49	59
200	57	68	73	88
300	70	89	101	116
400	87	109	118	148
500	117	141	156	172
No. of Mobile Nodes	**Network Lifetime (NL) (Rounds)**			
	QGSOC-SRP	FUCHAR	COBMA	EMPSO
100	5800	5300	5100	4890
200	5680	5260	5070	4600
300	5420	5100	4900	4560
400	5370	5060	4790	4200
500	5260	4800	4500	4140
No. of Mobile Nodes	**End to End (ETE) Delay (sec)**			
	QGSOC-SRP	FUCHAR	COBMA	EMPSO
100	3.12	4.93	5.96	6.67
200	3.65	5.68	7.46	8.77
300	4.09	6.38	8.56	9.97
400	5.04	7.58	9.36	11.67
500	5.23	8.78	9.96	12.77
No. of Mobile Nodes	**Throughput (Mbps)**			
	QGSOC-SRP	FUCHAR	COBMA	EMPSO
100	0.97	0.91	0.89	0.84
200	0.95	0.80	0.76	0.71
300	0.91	0.71	0.66	0.62
400	0.89	0.65	0.59	0.51
500	0.82	0.60	0.55	0.46

But the QGSOC-SRP model has surpassed all the other methods by obtaining least EC under all the mobile nodes. For example, in the presence of 100 nodes, the lowest EC of 31mJ has been attained by the QGSOC-SRP model whereas a higher EC of 45mJ, 49mJ, and 59mJ have been exhibited by the FUCHAR, COMBA, and EMPSO algorithms respectively. Accordingly, in the presence of 300 nodes, a minimum EC of 70mJ has been obtained by the QGSOC-SRP method but a superior EC of 89mJ, 101mJ, and 116mJ has been showcased by

the FUCHAR, COMBA, and EMPSO algorithms correspondingly. Eventually, in the presence of 500 nodes, the lowest EC of 117mJ has been achieved by the QGSOC-SRP model but a higher EC of 141mJ, 156mJ, and 172mJ has been demonstrated by the FUCHAR, COMBA, and EMPSO models respectively.

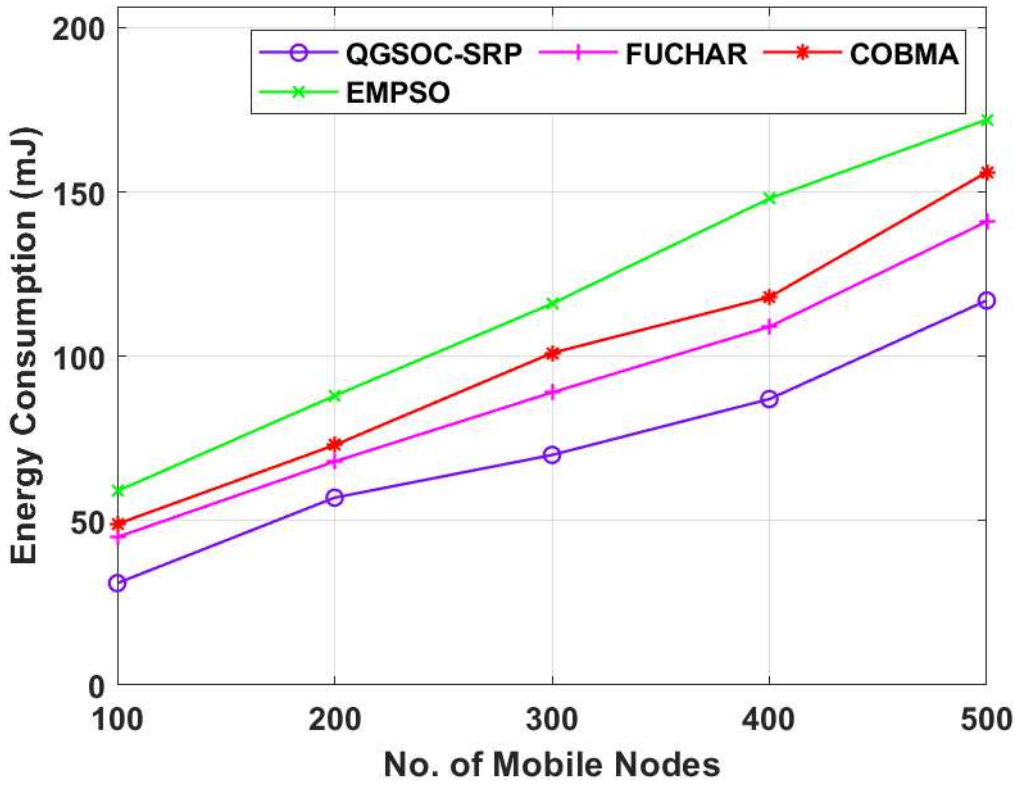

Fig. 6. Energy consumption analysis of QGSOC-SRP model

Fig. 7 analyses the NL performance of the QGSOC-SRP model under varying mobile node count. From the figure, it is observed that the EMPSO algorithm has failed to achieve better NL over the other algorithms. In the meantime, the COMBA and FUCHAR models have tried to report moderate network lifetime. However, the QGSOC-SRP model has showcased maximum NL. For instance, under the presence of 100 nodes, a maximum NL of 5800 rounds has been accomplished by QGSOC-SRP model whereas a minimum NL of 5300, 5100, and 4890 rounds have been depicted by the FUCHAR, COBMA, and EMPSO algorithms. Concurrently, under the presence of 300 nodes, the highest NL of 5420 rounds has been accomplished by QGSOC-SRP model while the lowest NL of 5100, 4900, and 4560 rounds have been showcased by the FUCHAR, COBMA, and EMPSO methodologies. At the same time, under the presence of 500 nodes, a superior NL of 5260 rounds has been accomplished by QGSOC-SRP model whereas a minimum NL of 4800, 4500, and 4140 rounds have been exhibited by the FUCHAR, COBMA, and EMPSO methods.

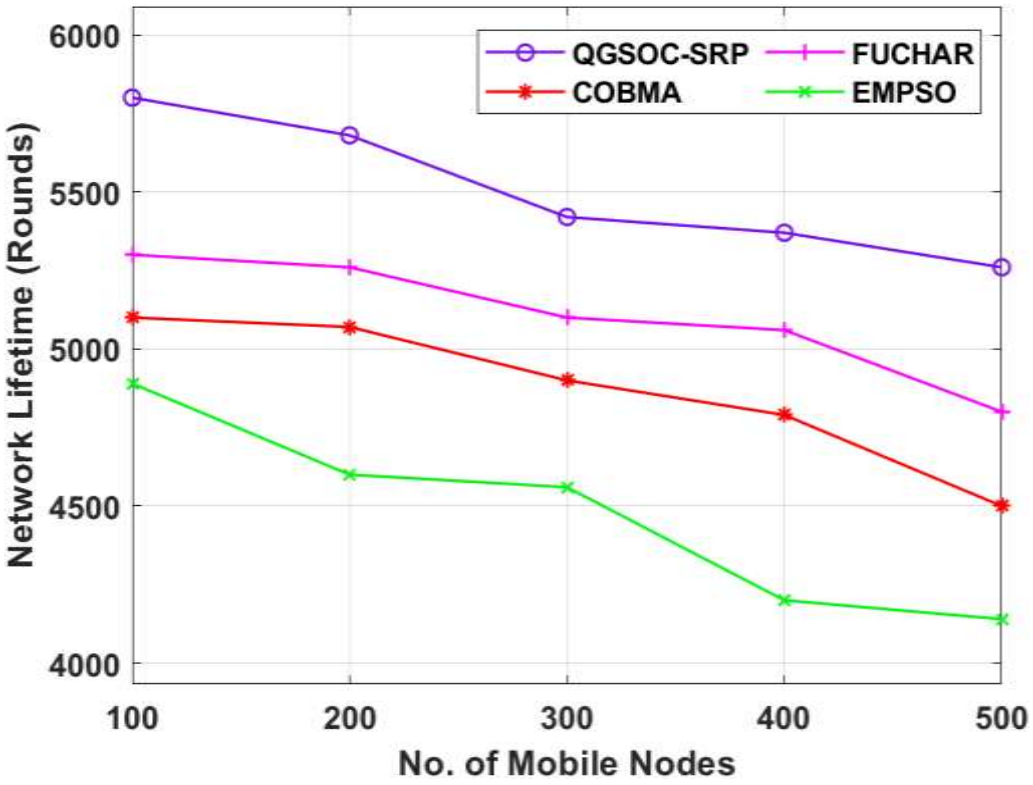

Fig. 7. Network Lifetime analysis of QGSOC-SRP model

Fig. 8 examines the ETE delay analysis of the QGSOC-SRP model under varying mobile nodes. The figure depicted that the EMPSO approach has shown showcased poor results by gaining maximum ETE delay. Similarly, the FUCHAR and COMBA methodologies have depicted moderate outcomes by providing better ETE delay over the EMPSO algorithm. However, the QGSOC-SRP method has outperformed the compared approaches by accomplishing minimum ETE delay under all mobile nodes. For instance, in the application of 100 nodes, minimum ETE delay of 3.12s has been achieved by the QGSOC-SRP model and maximum ETE delay of 4.93s, 5.96s, and 6.67s have been represented by the FUCHAR, COMBA, and EMPSO algorithms respectively. So, in the presence of 300 nodes, a minimum ETE delay of 4.09s has been reached by the QGSOC-SRP technique while a maximum ETE delay of 6.38s, 8.56s, and 9.97s has been demonstrated by the FUCHAR, COMBA, and EMPSO models respectively. Finally, in the presence of 500 nodes, the lowest ETE delay of 5.23s has been obtained by the QGSOC-SRP model but a superior ETE delay of 8.78s, 9.96s, and 12.77s have been showcased by the FUCHAR, COMBA, and EMPSO methodologies correspondingly.

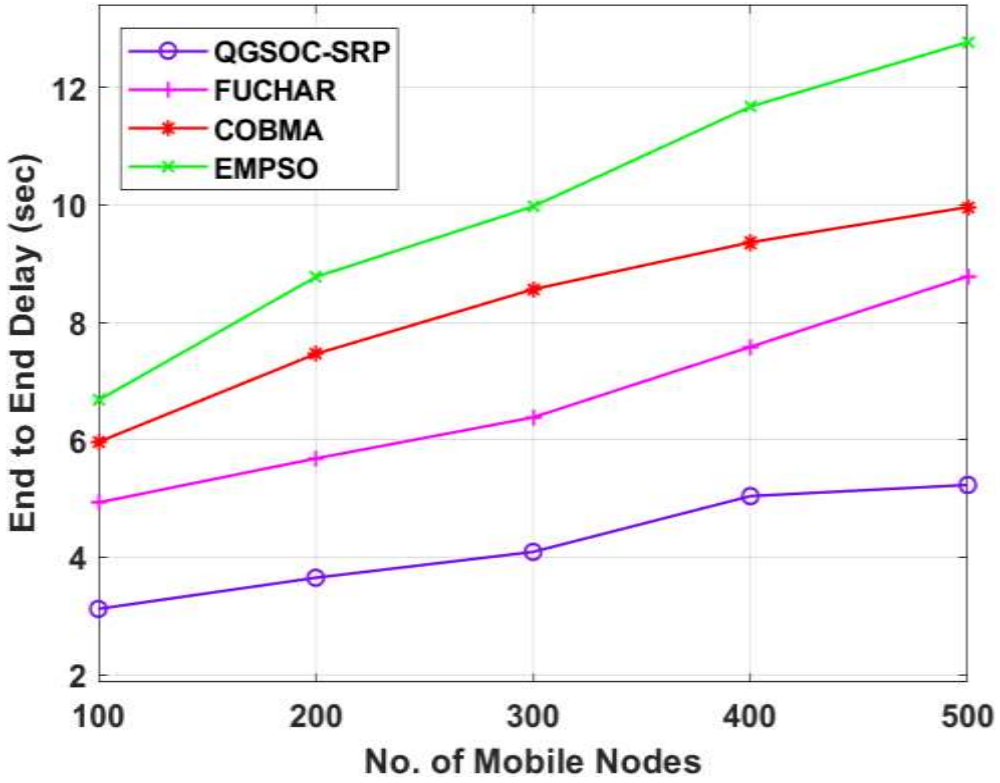

Fig. 8. ETE delay analysis of QGSOC-SRP model

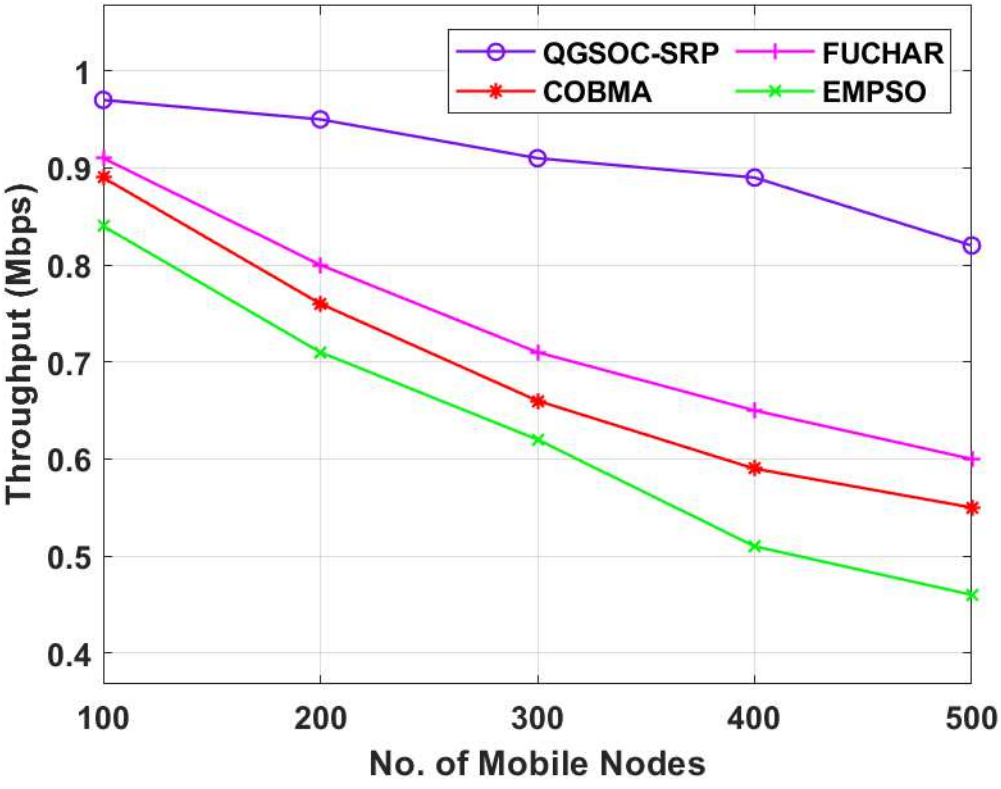

Fig. 9. Throughput analysis of QGSOC-SRP model

Fig. 9 inspects the throughput function of the QGSOC-SRP method under diverse mobile node count. From the figure, it is apparent that the EMPSO mechanism has failed to accomplish optimal throughput over the classical models. Simultaneously, the COMBA and FUCHAR methodologies have attempted to address considerable throughput. But, the QGSOC-SRP framework has displayed high throughput. For sample, under the existence of 100 nodes, a maximum throughput of 0.97Mbps is achieved by QGSOC-SRP model and minimum throughput of 0.91Mbps, 0.89Mbps, and 0.84Mbps have been illustrated by the FUCHAR, COBMA, and EMPSO algorithms. Simultaneously, under the presence of 300 nodes, a superior throughput of 0.91Mbps has been accomplished by QGSOC-SRP approach whereas a minimum throughput of 0.71Mbps, 0.66Mbps, and 0.62Mbps have been exhibited by the FUCHAR, COBMA, and EMPSO techniques. Likewise, under the presence of 500 nodes, the highest throughput of 0.82Mbps has been accomplished by QGSOC-SRP method but a minimum throughput of 0.60Mbps, 0.55Mbps, and 0.46Mbps has been portrayed by the FUCHAR, COBMA, and EMPSO models. From the detailed experimental analysis, it is evident the presented model achieves energy efficiency and maximizes network lifetime.

4. Conclusion

This paper has developed an effective QGSOC-SRP technique to achieve energy efficiency and prolong network lifetime in MANET. The presented QGSOC-SRP technique follows two-stage processes, namely optimal CH selection and route selection. The sensor nodes are initialized primarily and collect information about the surrounding environment. Then, the QGSOC algorithm gets executed by the BS to elect the CHs by the use of a FF involving four variables such as energy, distance, ND, and trust factor for the optimal election of secure CHs. Followed by, OGSA based routing technique is applied to pick up an optimal path to BS. Finally, the data will be transmitted from CMs to CHs and thereby to BS. To improve the effectiveness of the GSA, OGSA is derived based on the oppositional based learning concept for population initialization and generation jumping. The experimental validation of the presented model takes place in different aspects. The experimental outcome justified the superior performance of the presented model over the compared methods.

Funding Statement: The authors received no specific funding for this study.

Conflicts of Interest: The authors declare that they have no conflicts of interest to report regarding the present study.

Availability of data and material : Not Applicable

Code availability : Available based on Request

Authors' contributions : Maganti Srinivas – Article Preparation, Design, Implementation. Dr.M.Ramesh Patnaik- Conceptual Analysis, Design, Review and approval, Language Editing

References

[1] Hyland, M.; Mullins, B.E.; Baldwin, R.O.; Temple, M.A. Simulation-based performance evaluation of mobile ad hoc routing protocols in a swarm of unmanned aerial vehicles. In Proceedings of the 21st International Conference on Advanced Information Networking and Applications Workshops (AINAW'07), Niagara Falls, ON, Canada, 21–23 May 2007; Volume 2, pp. 249–256.

[2] Zhang, H.; Wang, X.; Memarmoshrefi, P.; Hogrefe, D. A Survey of Ant Colony Optimization Based Routing Protocols for Mobile Ad Hoc Networks. IEEE Access 2017, 5, 24139–24161.

[3] Sun, W.; Yang, Z.; Zhang, X.; Liu, Y. Energy-efficient neighbor discovery in mobile ad hoc and wireless sensor networks: A survey. IEEE Commun. Surv. Tutor. 2014, 16, 1448–1459.

[4] Polastre, J.; Szewczyk, R.; Mainwaring, A.; Culler, D.; Anderson, J. Analysis of wireless sensor networks for habitat monitoring. In Wireless Sensor Networks; Springer: New York, NY, USA, 2004; pp. 399–423.

[5] Tseng, Y.C.; Hsu, C.S.; Hsieh, T.Y. Power-saving protocols for IEEE 802.11-based multi-hop ad hoc networks. Comput. Netw. 2003, 43, 317–337.

[6] Doshi, S.; Bhandare, S.; Brown, T.X. An on-demand minimum energy routing protocol for a wireless ad hoc network. ACM SIGMOBILE Mob. Comput. Commun. Rev. 2002, 6, 50–66.

[7] Misra, A.; Banerjee, S. MRPC: Maximizing network lifetime for reliable routing in wireless environments. In Proceedings of the 2002 IEEE Wireless Communications and Networking Conference (WCNC2002), Orlando, FL, USA, 17–21 March 2002; Volume 2, pp. 800–806.

[8] Dressler, F.; Akan, O.B. A survey on bio-inspired networking. Comput. Netw. 2010, 54, 881–900.

[9] Bandgar, A.R.; Thorat, S.A. An improved location-aware ant colony optimization based routing algorithm for MANETs. In Proceedings of the 2013 Fourth International Conference on Computing, Communications and Networking Technologies (ICCCNT), Tiruchengode, India, 4–6 July 2013; pp. 1–6.

[10] Baras, J.S.; Mehta, H. A Probabilistic Emergent Routing Algorithm for Mobile Ad Hoc Networks. In Proceedings of the Modeling and Optimization in Mobile, Ad Hoc and Wireless Networks (WiOpt'03), Antipolis, France, 3–5 March 2003; 10p.

[11] Osagie, E.; Thulasiraman, P.; Thulasiram, R.K. PACONET: ImProved ant colony optimization routing algorithm for mobile ad hoc networks. In Proceedings of the 22nd International Conference on Advanced Information Networking and Applications (AINA 2008), Okinawa, Japan, 25–28 March 2008; pp. 204–211.

[12] Bullnheimer, B.; Hartl, R.; Strauss, C. A New Rank Based Version of the Ant System—A Computational Study; Vienna University of Economics and Business: Vienna, Austria, 1999; Volume 7, pp. 25–38.

[13] Woungang, I.; Dhurandher, S.K.; Obaidat, M.S.; Ferworn, A.; Shah, W. An ant-swarm inspired energy-efficient ad hoc on-demand routing protocol for mobile ad hoc networks. In Proceedings of the 2013 IEEE International Conference on Communications (ICC), udapest, Hungary, 9–13 June 2013; pp. 3645–3649.

[14] de Figueiredo Marques, V.; Kniess, J.; Parpinelli, R.S. An Energy Efficient Mesh LNN Routing Protocol Based on Ant Colony optimization. In Proceedings of the 2018 IEEE 16th International Conference on Industrial Informatics (INDIN), Porto, Portugal, 18–20 July 2018; Volume 1, pp. 43–48.

[15] Zhou, J.; Wang, X.; Tan, H.; Deng, Y. Ant Colony-Based Energy Control Routing Protocol for Mobile Ad Hoc Networks. In Proceedings of the International Conference on Wireless Algorithms, Systems, and Applications, Qufu, China, 10–12 August 2015; Springer: New York, NY, USA, 2015; pp. 845–853.

[16] Mohsen, A.M., 2016. Annealing ant colony optimization with mutation operator for solving TSP. *Computational Intelligence and Neuroscience*, *2016*.

[17] W.H. Liao, Y. Kao, Y.S. Li, A sensor deployment approach using glowworm swarm optimization algorithm in wireless sensor networks, Expert Syst. Appl. 38 (10) (2011) 12180–12188.

[18] Wang, D., Chen, H., Li, T., Wan, J. and Huang, Y., 2020. A novel quantum grasshopper optimization algorithm for feature selection. International Journal of Approximate Reasoning, 127, pp.33-53.

[19] Xiuwu, Y., Qin, L., Yong, L., Mufang, H., Ke, Z. and Renrong, X., 2019. Uneven clustering routing algorithm based on glowworm swarm optimization. Ad Hoc Networks, 93, p.101923.

[20] Rashedi E, Hossein Nezamabadi-pour, Saeid S. GSA: a gravitational search algorithm. Inform Sci 2009;179:2232–48.

[21] Tizhoosh HR. Opposition-based reinforcement learning. J Adv Comput Intell Intell Inform 2006;10(3):578–85

[22] Shaw, B., Mukherjee, V. and Ghoshal, S.P., 2012. A novel opposition-based gravitational search algorithm for combined economic and emission dispatch problems of power systems. International Journal of Electrical Power & Energy Systems, 35(1), pp.21-33.

[23] Selvi, M., Kumar, S.S., Ganapathy, S., Ayyanar, A., Nehemiah, H.K. and Kannan, A., 2020. An energy efficient clustered gravitational and fuzzy based routing algorithm in WSNs. Wireless Personal Communications, pp.1-30.

Figures

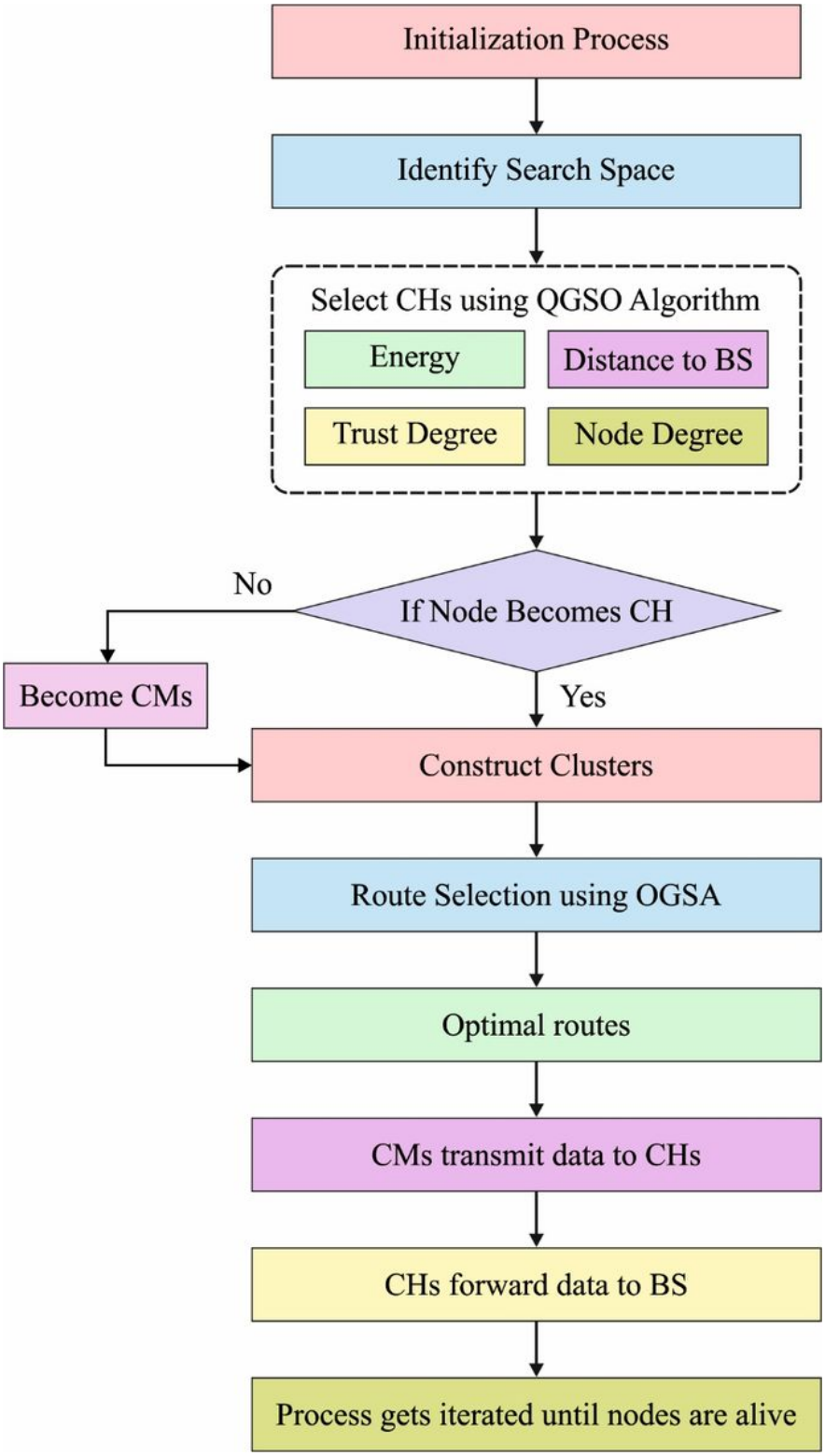

Figure 1

Work flow of QGSOC-SRP model

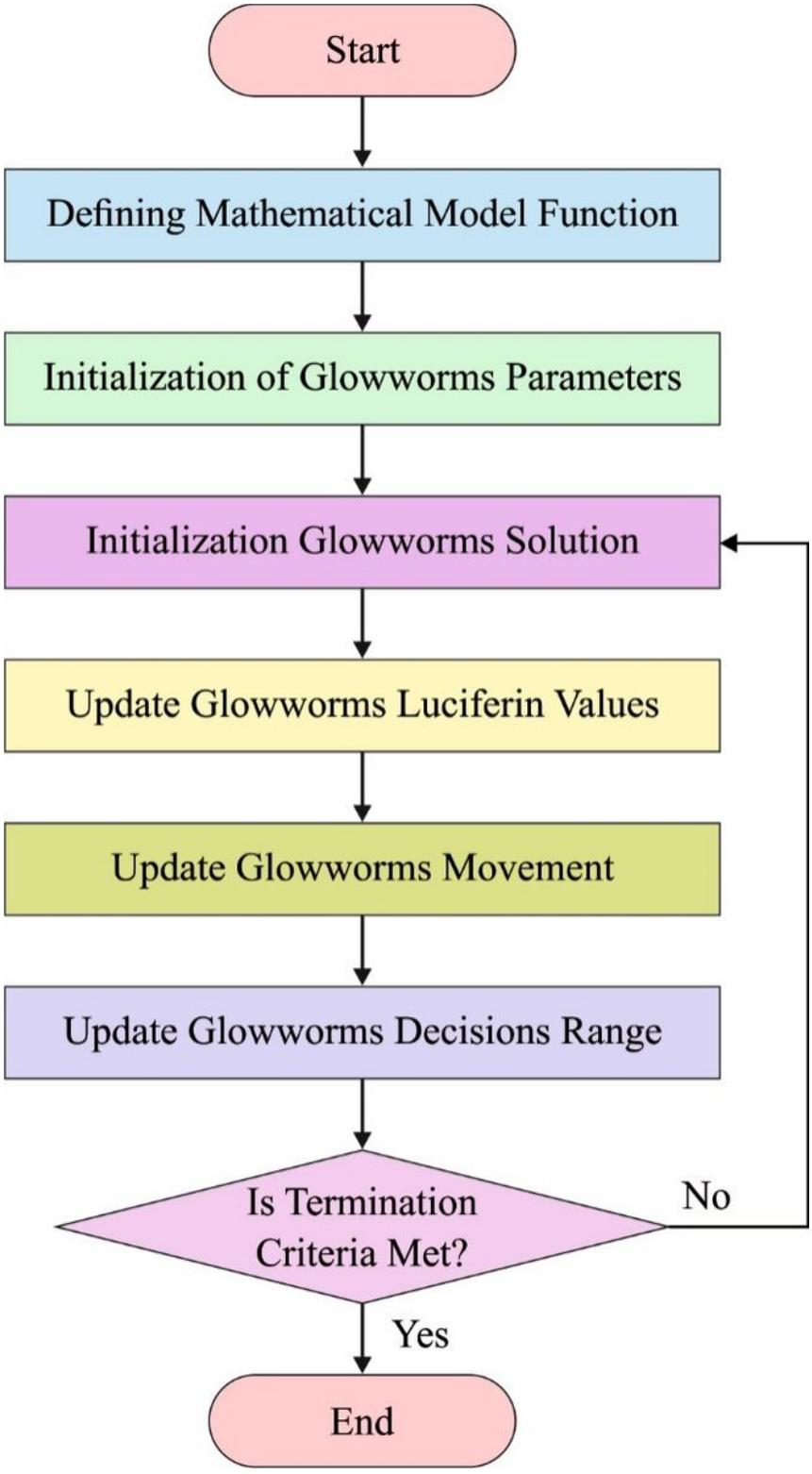

Figure 2

Flowchart of GSO algorithm

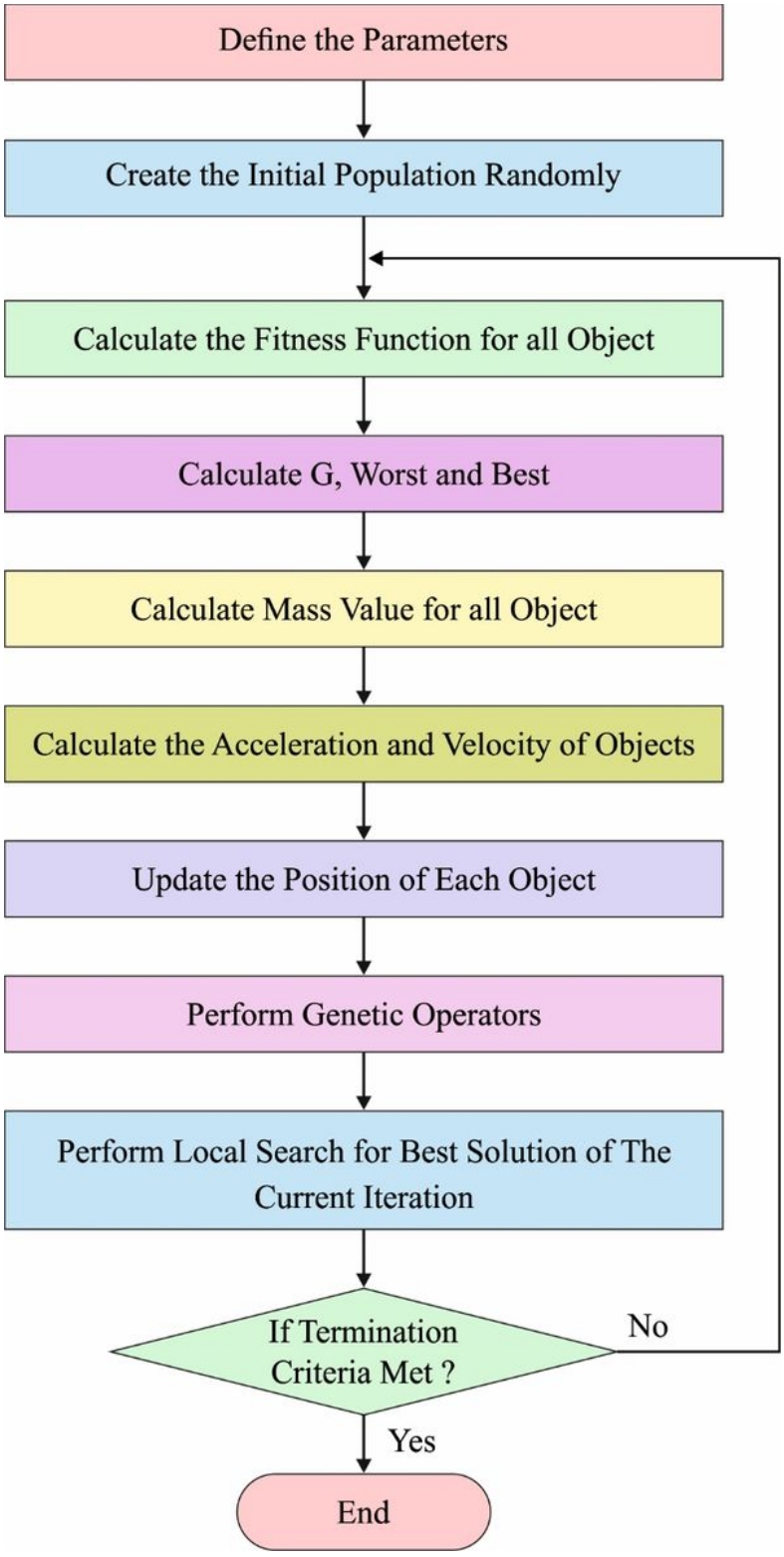

Figure 3

Flowchart of GSA algorithm

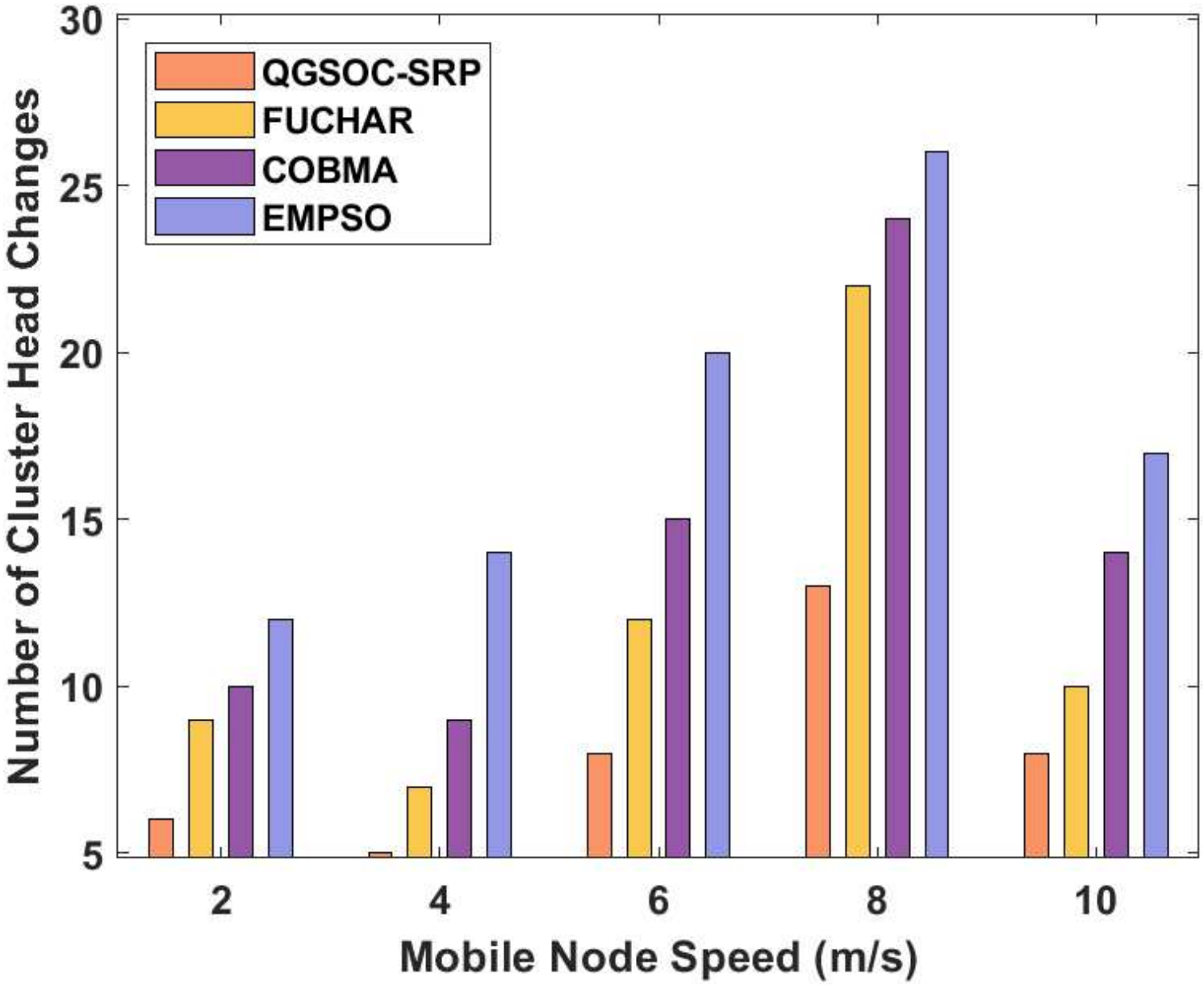

Figure 4

Results analysis of QGSOC-SRP model in number of cluster head

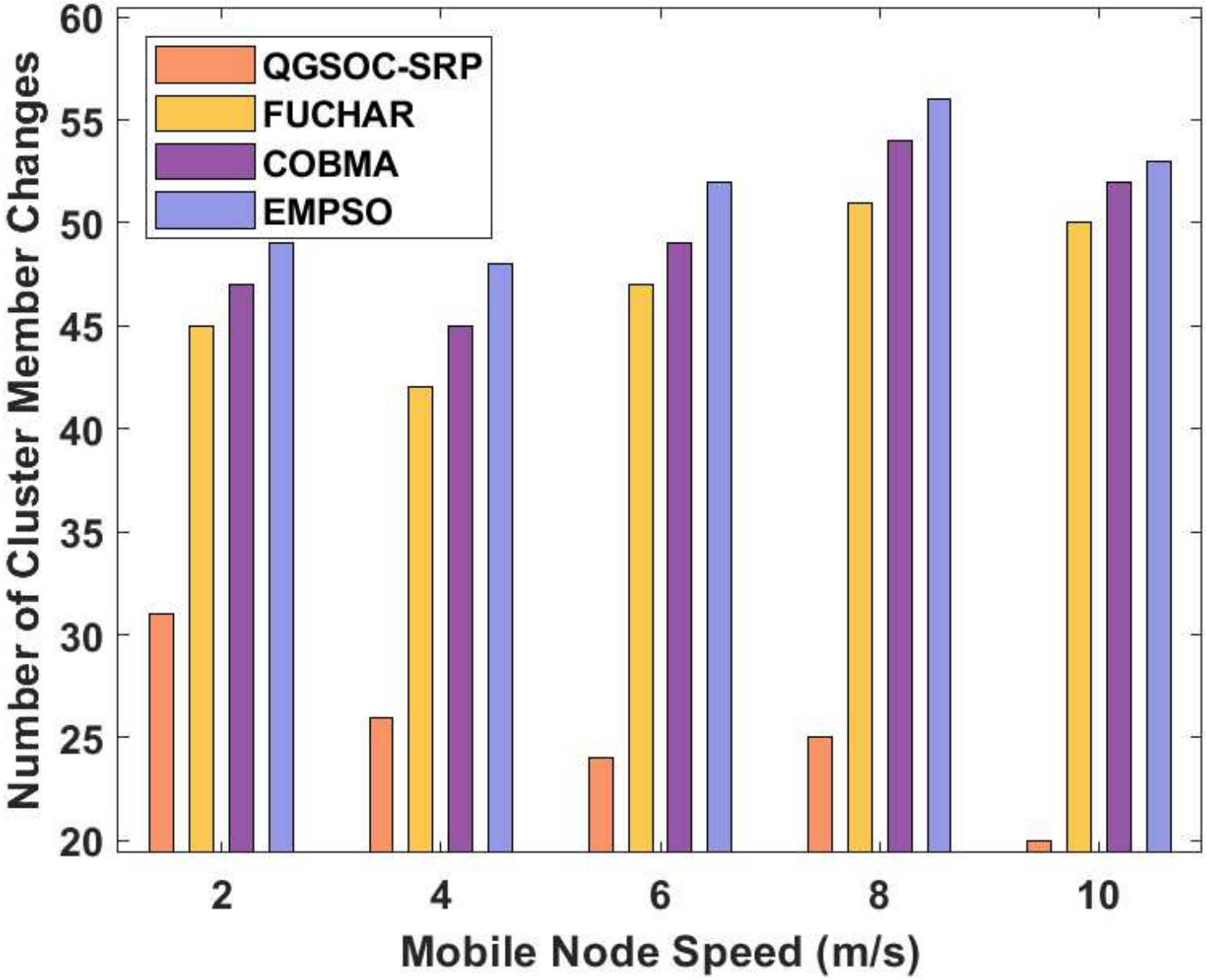

Figure 5

Results analysis of QGSOC-SRP model in number of cluster member

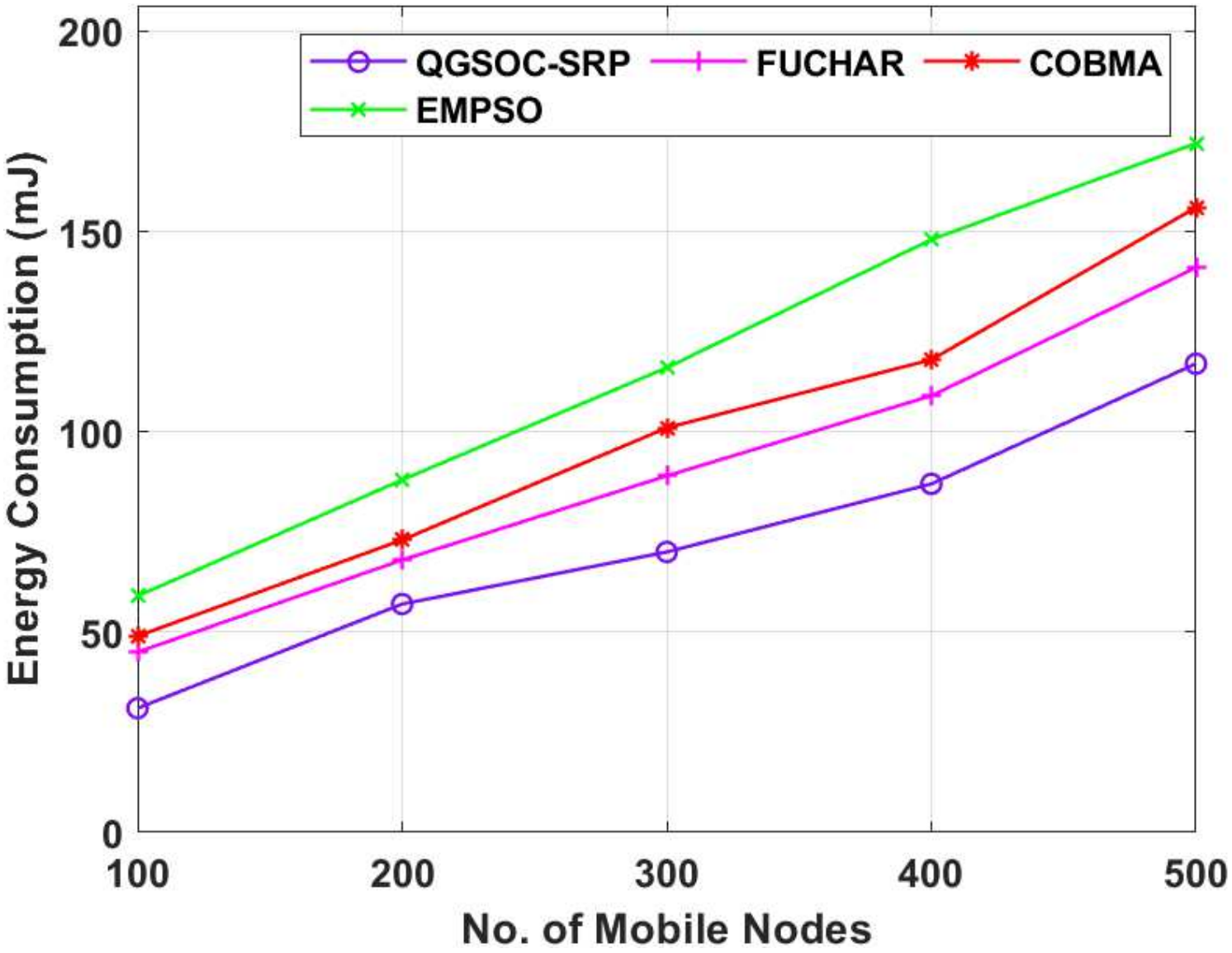

Figure 6

Energy consumption analysis of QGSOC-SRP model

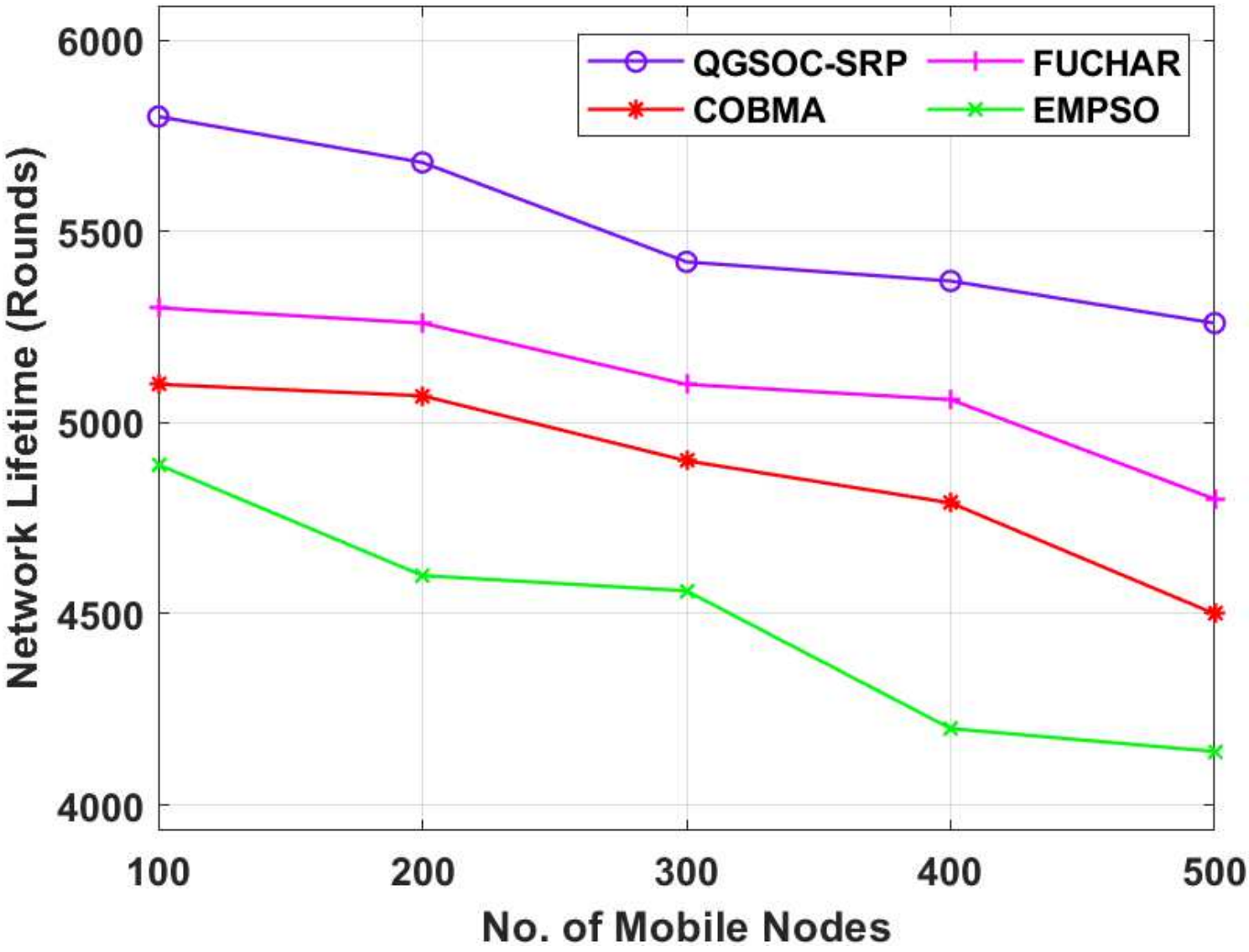

Figure 7

Network Lifetime analysis of QGSOC-SRP model

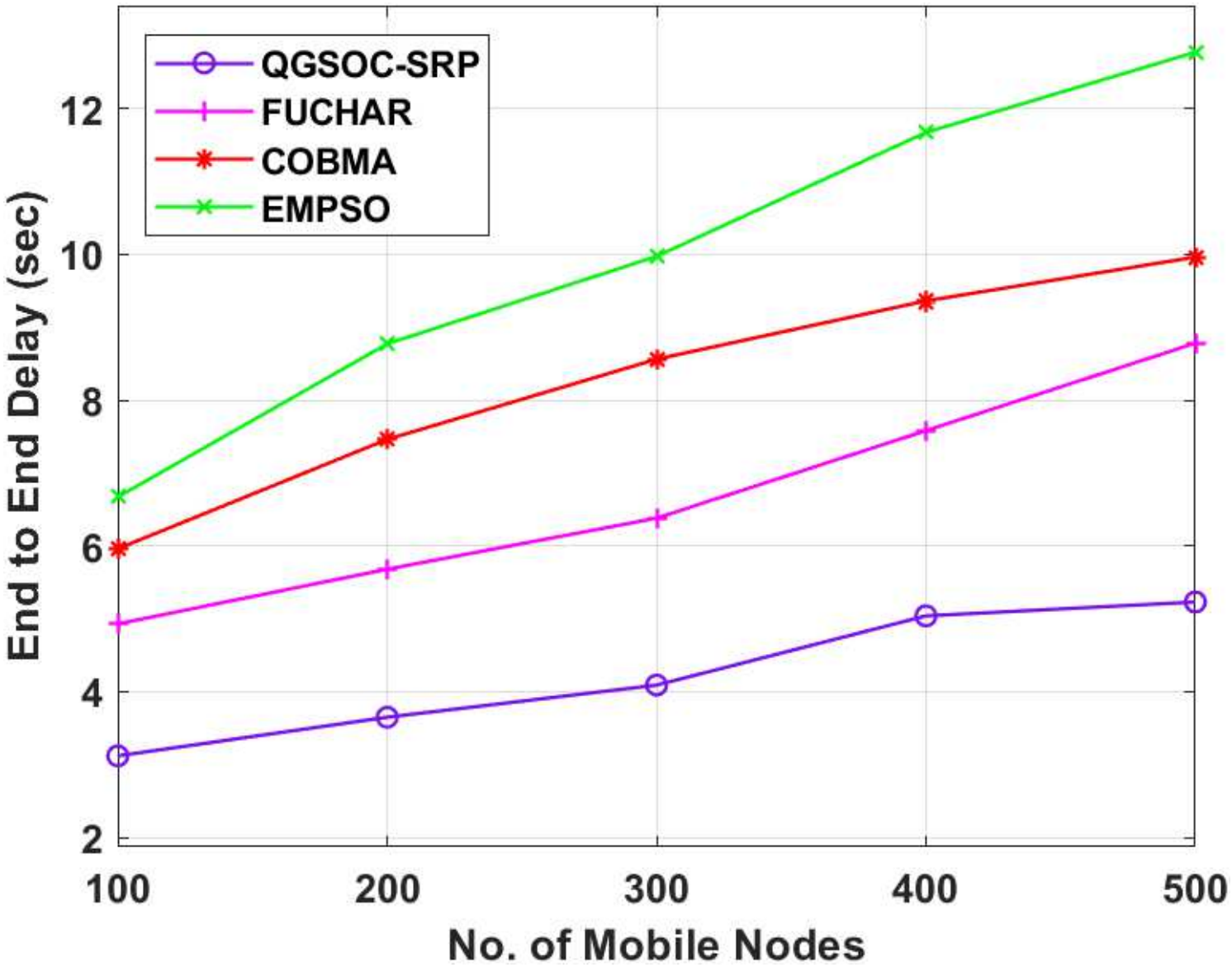

Figure 8

ETE delay analysis of QGSOC-SRP model

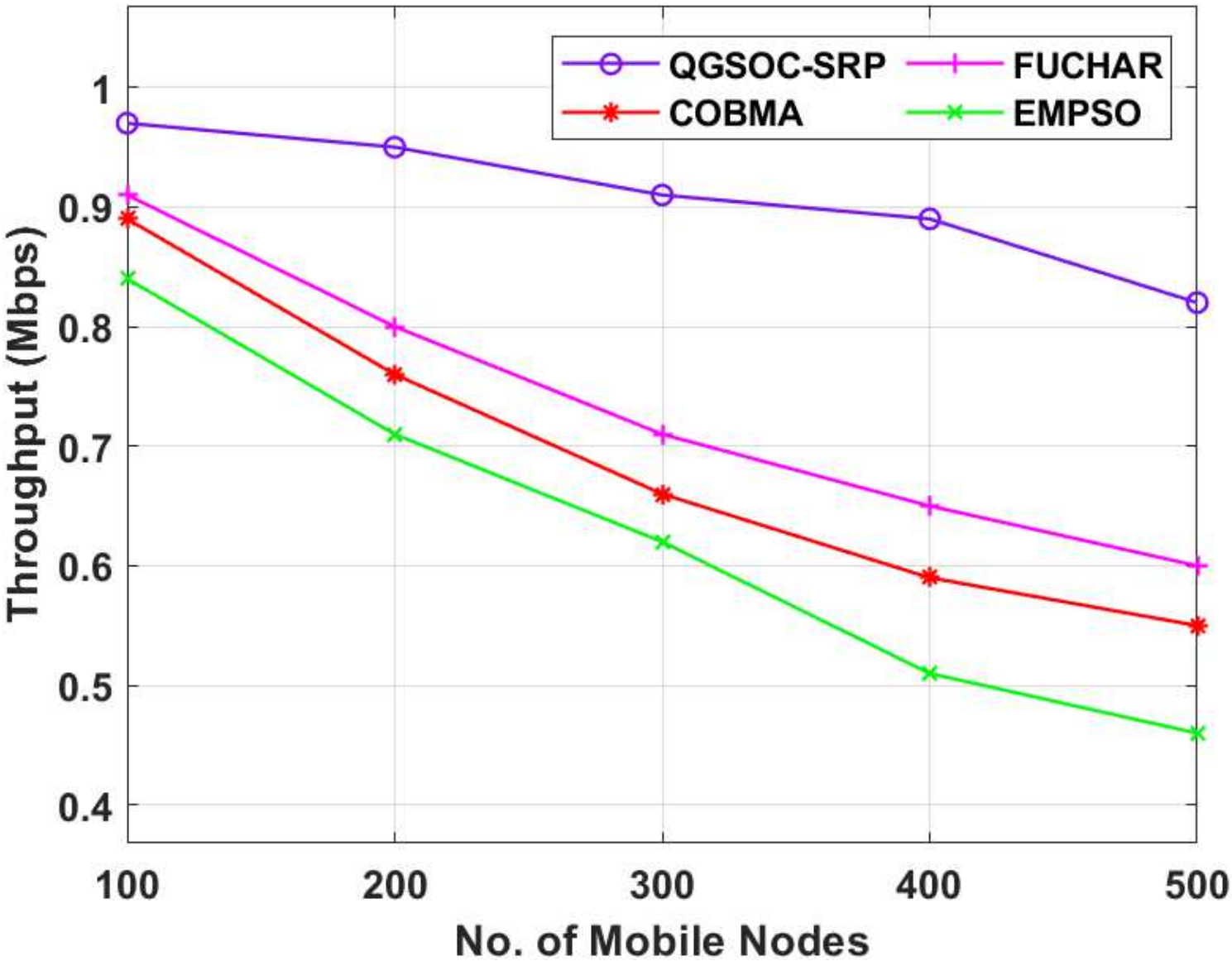

Figure 9

Throughput analysis of QGSOC-SRP model